Rain Attenuation Prediction Using Artificial Neural Network for Dynamic Rain Fade Mitigation

M. N. Ahuna, *Member, IEEE*, T. J. Afullo, *Senior Member*, *IEEE,* and A. A. Alonge, *Graduate Member, IEEE*

***Abstract*— Atmospheric processes from which rainfall is formed are complex and cannot be accurately predicted using mathematical or statistical models. In this paper, the backpropagation neural network (BPNN) is trained to predict rainfall rates, and hence attenuation that is likely to be experienced on a link. This study is carried out over the sub-tropical region of Durban, South Africa (29.8587°S, 31.0218°E). Utilizing the non-linear mapping capability between inputs and outputs, the backpropagation neural network is trained using rainfall data collected from 2013 to 2016 to predict rainfall rates. Long-term rain attenuation statistics arising from predicted rain rates are compared with actual and ITU-R model, and results show a relatively small margin of error between predicted rain attenuation exceeded for 0.01 % of an average year. Furthermore, analysis of predicted and actual rain attenuation within individual rain events from different rainfall regimes was carried out and results show that the proposed model can be used to predict the state of the link. This is demonstrated when the trained BPNN was tested using unseen data that was collected from January 2017 to May 2018, a period that spans through all four different climatic seasons of summer, autumn, winter and spring. Results of the test show a correlation coefficient of 0.8298. Finally, the proposed rain prediction model was tested on rainfall data from Butare, Rwanda (2.6078°S, 29.7368°E), which is a tropical region and results obtained indicate the portability of the proposed model to other regions.**

***Index Terms*—artificial neural network, backpropagation neural network, rain attenuation, rain rate**

I. Introduction

Satellite and terrestrial microwave links operating at frequencies above 10 GHz may suffer from signal outages during a heavy rainfall event [1-4]. Continuous streaming of content may thus be compromised during point-to-point (PP) communication. Live streaming of content like prime news and sport events demand virtually zero link outages. Rainfall is a natural phenomenon that attenuates the signal along the wireless communication link and, therefore, it becomes mandatory to mitigate rain attenuation for continuous content streaming. On this premise, dynamic fade mitigation techniques can be employed in conjunction with fade prediction models which are capable of predicting the state of the link. Accordingly, measures can be taken to ensure that the link is fully available for communication even in the advent of a rainfall storm event. Many researchers, including [5-8], have used an artificial neural network (ANN) for rainfall forecasting, and showed that the ANN can give acceptable results after training. In this paper, a backpropagation neural network (BPNN) is used to predict and classify rain attenuation for dynamic rain attenuation mitigation.

This paper is a detailed extension of work originally reported in [8]. In the current paper, additional material include: (1) retraining the BPNN with complete 2016 data, contrary to [8] where some data was set aside for testing and validation of the training network; (2) generation of CCDFs for predicted rain rates and rain attenuation, and (3) classification of predicted rain attenuation. The paper is structured as follows: Section 2 gives a summary of related work whereas Section 3 describes the artificial neural network as a computing unit. In Section 4, the methodology of this work is given while in Section 5 the analysis of results is carried out. The proposed prediction model is validated in Section 6 and the work is concluded in Section 7.

II. Related Work

Studies on the application of artificial neural networks in the prediction of rainfall and rainfall rates have been on the rise, with most applications geared towards the field of water management and meteorology [6, 9-12]. *French et al.* [13] used an artificial neural network in forecasting a 2-dimentional rainfall one hour in advance. Their work became a good ground for most researchers to lay and advance studies in this area.

In 1995, *Michaelides et al.,* [9] used an ANN in conjunction with daily rainfall observations in the neighboring sites to estimate missing rainfall data over Cyprus. *Christodoulou et al.,* [5] trained the self-organizing map (SOM) and K-Nearest Neighbor (KNN) machine learning classifiers using radar data as inputs and rain gauge data as outputs to predict rainfall rate in Italy.

III. The Artificial Neural Network Computing Tool

The neural network as a computing unit is divided into two functional parts: an integration function part, which sums the *N* inputs into a single value; and the output (or activation) function, which produces an output in accordance with the function of computation. The common activation function is the sigmoid function which possesses two beneficial properties namely: (1) continuity and, (2) differentiability of the error function during training. A simplified diagram of this computing unit and the training structure are shown in Fig. 1 and Fig. 2, respectively.

M. N. Ahuna and T. J. Afullo are with University of KwaZulu-Natal, Duban, South Africa (email: mary.ahunah@gmail.com; afullot@ukzn.ac.za).
A. A. Alonge is with University of Johannesburg, Johannesburg, South Africa (email: aalonge@uj.ac.za).

Integration and activation functions shown in Fig. 1 are given by [8, 14]:

$$g = b + \sum_{n=1}^{N} w_n i_n \qquad n = 1,2,\ldots,N \tag{1}$$

$$f(g) = \frac{1}{1+e^{-g}} \tag{2}$$

where g is the integration function, b is the bias input, f is the activation function, N is the number of inputs, w_n is the nth weight and i_n is the nth input.

The actual output of the BPNN is obtained by the application of the activation function to the summation function as shown in (2). Thereafter, evaluation of the network's performance is done during training by computing an error, E, given by [14, 15]:

$$E = \frac{1}{2}\sum_{h=1}^{H}(O_t - O_a)^2 \tag{3}$$

where O_a is the actual output, O_t is the desired output (target) and H is the number of data points. Errors in (3) are minimized using an error derivative given by [8, 14]:

$$\frac{\partial E_{total}}{\partial O_a} = -(O_t - O_a) \tag{4}$$

An optimized weight vector, w, that provides a minimized error function is achieved by updating associated weights using the expression,

$$\Delta w_i = \eta \frac{\partial E}{\partial O_i} \qquad i = \quad 1,2,\ldots,I \tag{5}$$

where η is the learning rate, i is the input, Δw_i is the weight change on the ith input and O_i and the output contributed by the ith input.

The main objective in (3) is to find a minimized error function with $\nabla E = 0$ for prediction of a future rainfall rate $R_p(t+1)$ mm/h, given by [8]:

$$R_p(t+1) = f\big(R_a(t-2), R_a(t-1), R_a(t)\big) \tag{6}$$

where $R_a(t)$ is the actual rainfall rate at time t, $R_a(t-1)$ is the actual rain rate at time $(t-1)$, $R_a(t-2)$ is the actual rain rate at time $(t-2)$. All rain rates being in mm/h.

Most rain rate prediction models predict rain rates exceeded at various percentages of time in an average year. Some of these models include the work of [16] and [17]. For rain attenuation prediction, various prediction models have been proposed and include Bryant model [18], SC EXCELL model [19], Crane two-component model [20], SST model [21] and ITU-R model [22].

In this study, the SST model proposed by *Matricciani* [21] and the ITU-R model [22] are used for prediction of attenuation due to rain. For the model proposed in [21], the vertical structure of rain is modelled as two layers of precipitation, layer A (hydrometeors in the form of rain drops) and layer B (melting hydrometeors). In addition, the ITU-R P.618-13 also provides a model for prediction of rain attenuation exceeded for different percentages of time in an average year. This model is given in [22]:

$$A_p = A_{0.01}\left(\frac{p}{0.01}\right)^{-0.655+0.033\ln(p)-0.045\ln(A_{0.01})-\beta(1-p)sin\theta} \tag{7}$$

and:

$$A_{0.01} = kR_{0.01}{}^{\alpha} \times L_{eff} \qquad [dB] \tag{8}$$

where p is the probability of exceedance in %, A_p is the attenuation exceeded p % of time in an average year, $A_{0.01}$ is the attenuation exceeded 0.01 % of time in an average year, β is the parameter dependent on the latitude of the earth station, and θ is the angle of elevation of the earth station antenna, and L_{eff} is the effective slant path length, with both β and θ as obtained in [22], k and α are parameters dependent on frequency.

Rain attenuation time series obtained from the SST model proposed by [21] is given by:

$$A(t) = k_A R(t)^{\alpha_A} L_A + r^{\alpha_B} k_B R(t)^{\alpha_B}(L_B - L_A) \tag{9}$$

where $A(t)$ is rain attenuation, in dB, at time t, L_A and L_B are precipitation layer and the melting layer slant paths, respectively, in km, $R(t)$ is the rain rate in layer A, r is rain rate in layer B whose value is given in [21], whereas k_A, α_A, k_B, and α_B are frequency-dependent parameters for layer A and layer B given in [23].

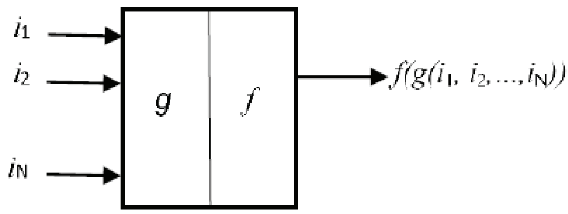

Fig. 1 ANN Computing unit

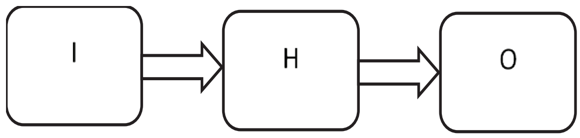

Fig. 2 BPNN training structure

IV. METHODOLOGY

Data for training and validating the BPNN model proposed in this work was collected at the University of KwaZulu-Natal, Durban, through a JWD, RD-80 impact type disdrometer with a sampling time of 30 seconds. Additional details and setup are given in [4, 8]. Training data was collected for a period of four years from 2013 to 2016. This dataset comprises of four rainfall regimes from drizzle to super storms and the total number of training samples used was 108,861. Validation and testing data was drawn from data collected from January 2017 to May 2018.

Rainfall data within this period of 17 months are a representation of all four seasons (summer, autumn, winter and spring) that are experienced in South Africa.

V. RESULTS AND ANALYSIS

This section presents the analysis of results that were obtained from the study.

A. BPNN Training

A three-layered network with three neurons in the input layer (I), three neurons in the hidden layer (H) and one neuron in the output layer (O) was used during training as shown in Fig. 2. This architectural structure is simplified as 3:3:1:1, where the last '1' represents the network output and not a neuron.

The artificial neural network was trained using TRAINLM training function and LEARNGDM as the adaptation learning function. Performance functions chosen were the mean squared error (MSE) and TANSIG transfer function. Training, testing and validation results are shown in Fig. 3 and Fig. 4.

During the neural network training, the best performance reached was the optimum mapping of outputs and targets at epoch 371 of 377 epochs with a mean square error of 6.017. The training performance plot is shown in Fig. 3. Similarly, Fig. 4 shows the training regression plot with a regression coefficient, R^2 = 0.91094 which shows a good correlation between the actual outputs and predicted outputs.

Optimized weight and bias matrices that were obtained during the training process are shown in (10).

$$w_{\mathrm{HI}} = \begin{bmatrix} -0.1974 & -1.1467 & -7.8568 \\ -0.0115 & 0.0086 & -0.0476 \\ 4.0797 & 6.1838 & 6.0543 \end{bmatrix} \quad (10a)$$

$$w_{\mathrm{OH}} = [-78.4395 \quad -32.0736 \quad 31.939] \quad (10b)$$

$$b_{\mathrm{H}} = \begin{bmatrix} -11.4485 \\ 0.4845 \\ -17.3805 \end{bmatrix} \quad (10c)$$

$$b_{\mathrm{O}} = [-32.1027] \quad (10d)$$

where w_{HI} is the weight vector for weights from the input to the hidden layer, w_{OH} is the weight vector for weights from the hidden layer to the output layer, b_{H} is the input bias vector to the hidden layer, and b_{O} is the bias input to the output layer.

In Fig. 5, the unseen model testing dataset was sourced from 2017-2018 rainfall data. This data is 'unseen' to the trained network because it was not used during training. Results of testing show a fair correlation of R^2 = 0.8298. Further, this complete model testing dataset was compared to the output of the trained neural network and an overall root mean square error (RMSE) value of 2.5128 was realized. Fig. 6 shows the correlation between the ANN predicted output and the current or actual output. The correlation between these two outputs is 0.9811. This correlation implies that the current output can be used to predict a future rain rate at time $(t + 1)$. This prediction can be deduced from the relationship shown in Fig. 6 and is given by:

$$R_p(t+1) = mR_a(t) + n \quad (11)$$

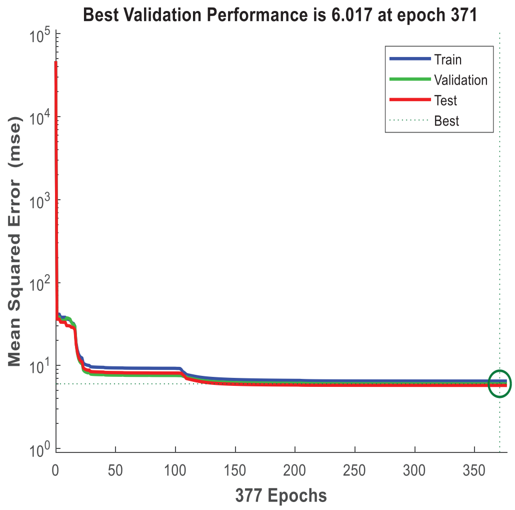

Fig. 3 BPNN training performance plot

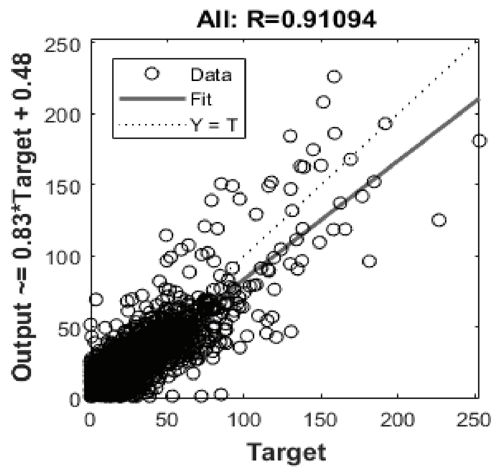

Fig. 4 BPNN training regression plot

where m and n are regression parameters whose values are 0.9036 and n = 0.3483, respectively. Consequently, from (9) and (11), link attenuation at time $(t + 1)$ can be predicted by:

$$A_p(t+1) = \Phi L_A + \Psi(L_B - L_A) \quad (12a)$$

with:

$$\Phi = k_A R_p(t+1)^{\alpha_A} \quad (12b)$$

$$\Psi = r^{\alpha_B} k_B R_p(t+1)^{\alpha_B} \quad (12b)$$

B. Complementary cumulative distribution functions

CCDFs aid in the determination of acceptable link fade margins by providing information on different percentages of parameter exceedances for an average year. For system design engineers, the parameter of ultimate importance is the rain rate exceeded for 0.01 % ($R_{0.01}$) and 0.001 % ($R_{0.001}$) of time in an average year [4, 24, 25]. In this paper, rain rate and rain attenuation CCDFs are derived from rainfall data collected

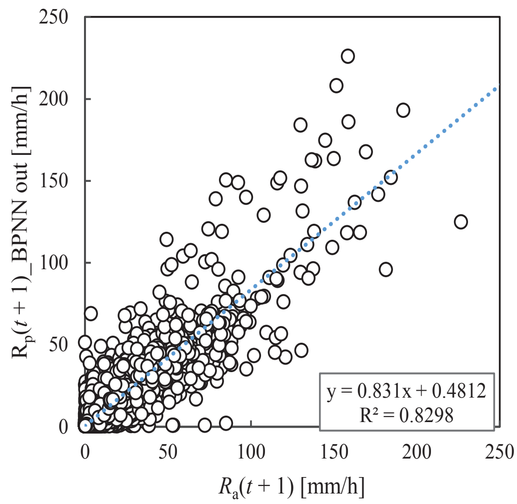

Fig. 5 Correlation between BPNN predicted outputs with actual output

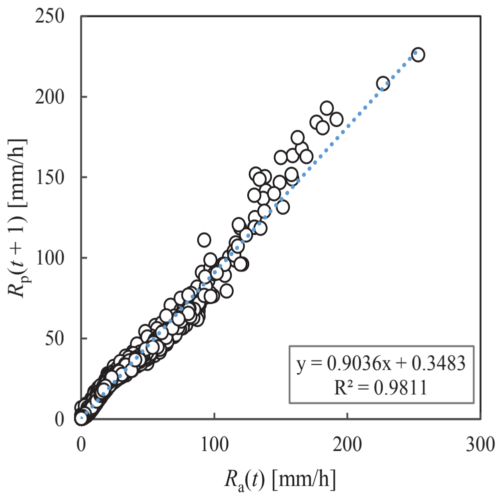

Fig. 6 Correlation between BPNN predicted outputs with current rain rate

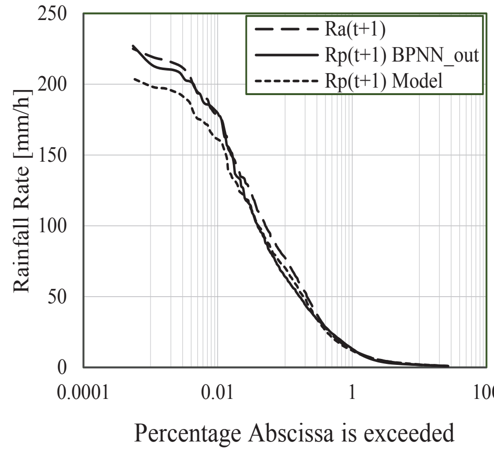

Fig. 7 Rain rate CCDFs (2017-2018)

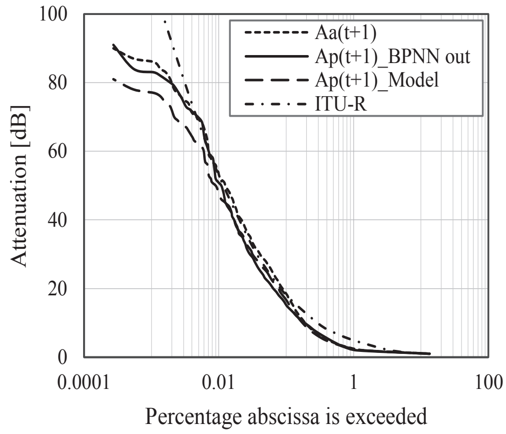

Fig. 8 Rain attenuation CCDFs (2017-2018)

TABLE I
RAIN RATE EXCEEDED

%	R_a(t+1) [mm/h]	R_p(t+1) BPNN out [mm/h]	R_p(t+1) model [mm/h]
1	12	13	12
0.1	77	64	70
0.01	177	178	160
0.001	219	213	198

TABLE II
RAIN ATTENUATION EXCEEDED

%	$A_a(t+1)$ [dB]	$A_p(t+1)$ BPNN out [dB]	$A_p(t+1)$ model [dB]	$A_p(t+1)$ *ITU-R* [dB]
1	2	2	2	5
0.1	18	15	16	18
0.01	53	50	48	53
0.001	86	83	77	106

from January 2017 to May 2018. Fig. 7 and Table I shows long-term rain rate statistics for actual rain rates, ANN predicted rain rates and modelled rain rates. In Fig. 7, it is seen that rain rates exceeded for various percentages of time in an average year are close for the three distributions for percentages below 0.01. For the ANN output, the values are close to actual values for almost all percentages.

From Fig. 7, it is seen that the rainfall rate exceeded for 0.01 % of time in an average year is 177 mm/h and 178 mm/h for actual and predicted outputs, respectively. For the model, this value is 160 mm/h. Similarly, Fig. 8 and Table II show resultant long-term rain attenuation statistics for both actual and predicted rainfall rates.

The ITU-R rain attenuation model is also included for comparison of exceedances at various percentages. It is revealed that attenuation exceeded for 0.01 % of an average year is 53 dB (actual rain rates), 50 dB (ANN predicted rain rates), 48 dB (proposed model) and 53 dB (ITU-R model).

VI. Rain attenuation prediction and Prediction Model validation

The applicability of the trained neural network and the proposed model was tested on different rainfall events from different rainfall regimes. Five attenuation classes with attenuation thresholds at 10 dB, 20 dB, 40 dB and 60 dB were used to show the suitability of the proposed model in the prediction of rainfall attenuation for dynamic rain fade mitigation. These attenuation classes are shown in Table III.

Tests on the trained prediction model were carried out on individual rain events across different rain regimes. For instance, Fig. 9(a) shows the comparison of predicted and actual rain rate time series. In this figure, rain rate times series within a rain event with a maximum rain rate of 22.2265 mm/h was tested against ANN predicted outputs and model outputs.

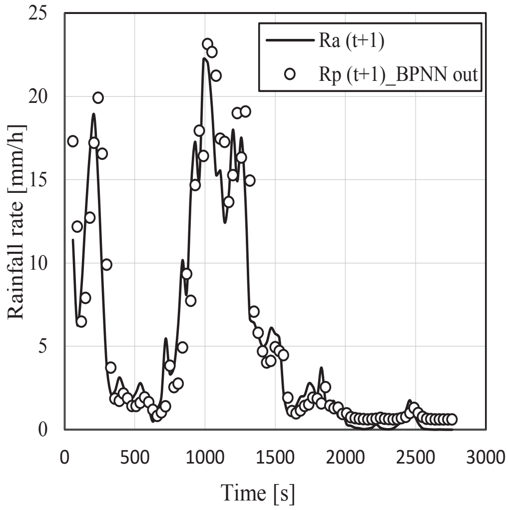

(a)

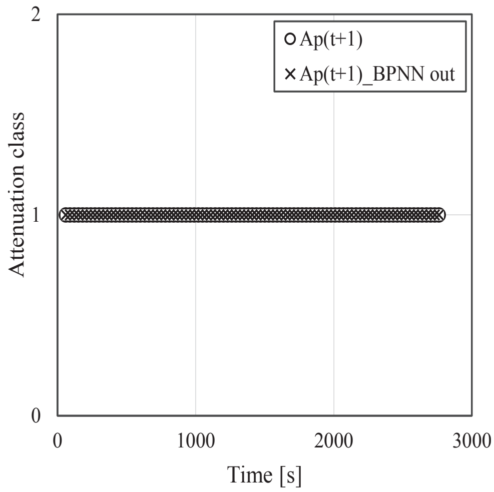

(b)

Fig. 9 (a) Rain rate prediction (BPNN out) (b) classification of predicted attenuation levels for storm event of 15th May, 2017, 23:03:30 hours

Using attenuation classifications shown in Table III and Fig. 9(b), we show that the predicted rain attenuation values are within the expected bound of $A < 10$ dB (Level 1). A good agreement is observed when the 'o' and 'x' markers merge on the graph as seen in Fig. 9(b).

Similarly, Fig. 10(a) and Fig. 10(b) show rain rates and attenuation comparison between the model output and actual outputs. Once more, the model attenuation class outputs are within expected classes.

In Fig. 11(a), the model output is tested on a rain event with a maximum rain rate of 89.9575 mm/h. From this rain event, there are three attenuation levels, 1-3, with a few misses in the predicted rain attenuation as seen in Fig. 11(b). Fig. 12 shows

TABLE III
Rain Attenuation Classes

Attenuation Class	Class Bounds [dB]
1	$A < 10$
2	$10 \leq A < 20$
3	$20 \leq A < 40$
4	$40 \leq A < 60$
5	$A \geq 60$

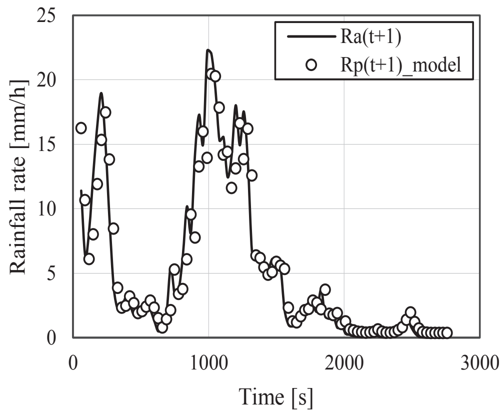

(a)

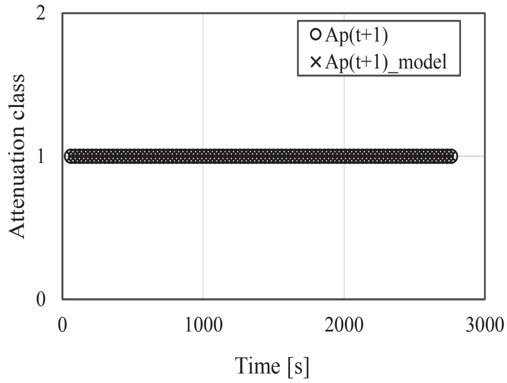

(b)

Fig. 10 (a) Rain rate prediction (model) (b) classification of predicted attenuation levels for Storm event of 15th May, 2017, 23:03:30 hours

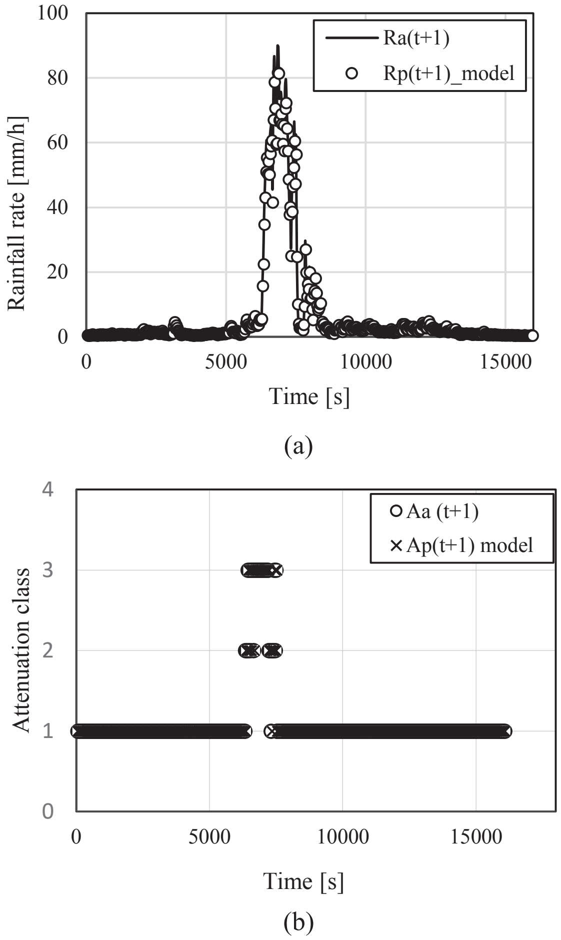

Fig. 11 (a) Rain rate prediction (model) (b) classification of predicted attenuation levels for Storm event of 21st Feb. 2018, 20:29:00 hours

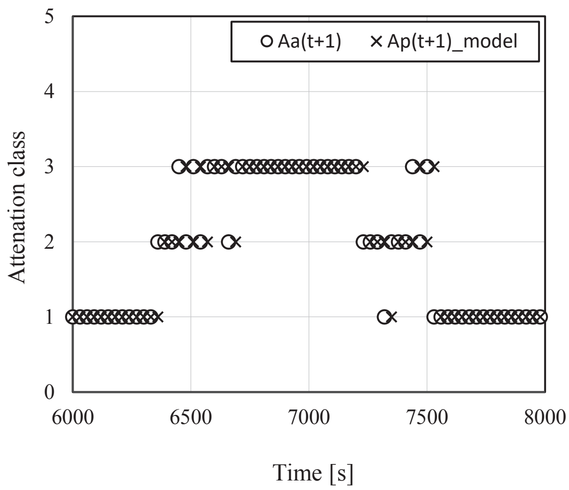

Fig. 12 Detailed attenuation classification of predicted attenuation levels in Fig. 11(b)

a detailed section of Fig. 11(b), spanning 600 seconds. Within the testing dataset, the highest rain rate observed was 224.9989 mm/h within a rain event of 22nd February, 2017 at 10:53:00

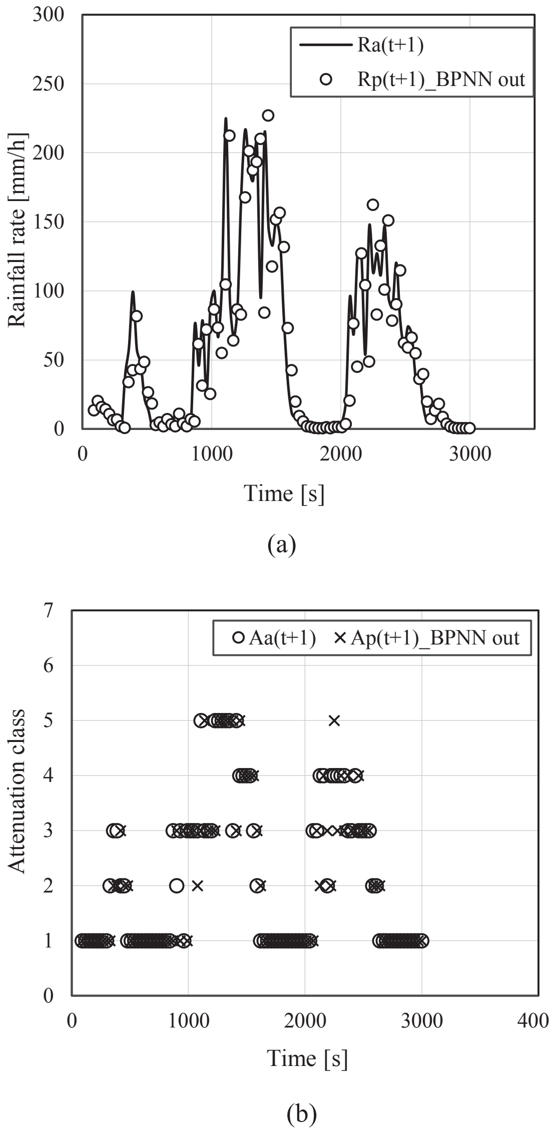

Fig. 13 (a) Rain rate prediction (model) (b) classification of predicted attenuation levels for Storm event of 22nd Feb. 2017, 10:53:00 hours

hours, over Durban. This event is shown in Fig. 13(a). In this figure, it is seen that five attenuation levels are obtained up to the highest attenuation class of level 5. A view of a detailed section of Fig. 13(b) is shown in Fig. 14, in which there are nine misses during the period of deep fading within 600 s from time t = 1000 s to t = 1600 s. However, cases where the 'x' marker is above the 'o' maker can be considered safer because during these instances, attenuation is overestimated, which means that a fade mitigation measure will be effected. Additionally, further analysis shows that overestimation or underestimation of these rain attenuation, in most cases, involves two adjacent levels. Additional analysis shows that instances of sharp spikes are rare and short-lived. More importantly, these results show that the ANN model is able to predict deep fades on the link (Level 5) as seen in Fig. 14.

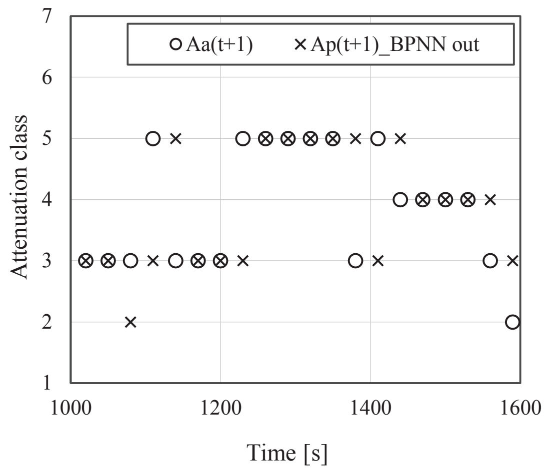

Fig. 14 Detailed attenuation classification of predicted attenuation levels in Fig. 13(b)

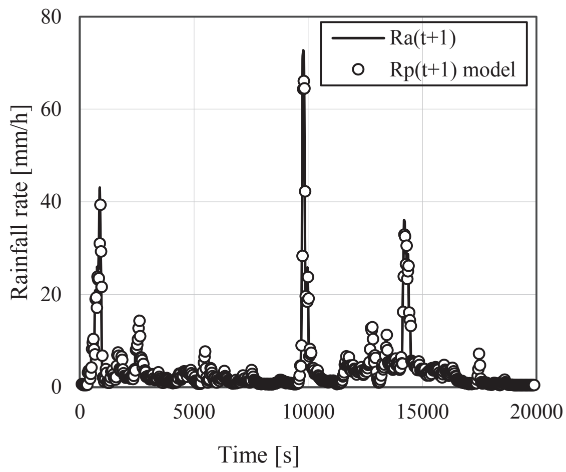

(a)

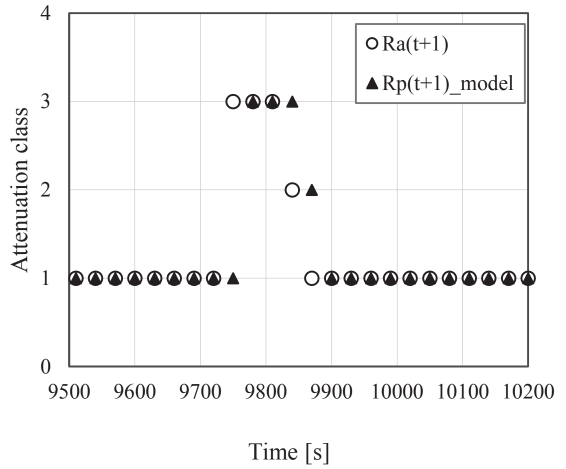

(b)

Fig. 15 (a) Rain rate prediction (model) (b) classification of predicted attenuation levels for storm event of 17th Feb. 2015, 10:31:00 hours in Butare, Rwanda

To ascertain the portability of the proposed model, rainfall data sampled at 1-minute integration time was used to test the model with a rain event from Butare, Rwanda, a region with equatorial climate. Results of this test are shown in Fig. 15. Analysis of this test is presented in Fig. 15(b) and shows that there are three misses within a period of 600 s, which, excluding overestimation, reduces to only one miss for a case of underestimation at time $t = 9750$ s.

VII. Conclusion

This study has established that a backpropagation neural network can satisfactorily be used to predict the state of the link during a rainfall event for dynamic rain fade mitigation. Results show that the trained backpropagation neural network is able to predict deep fades sufficiently well during a super storm rain event. Additionally, the proposed model can be portable to other locations with different geographical climates, provided that the sampling time is relatively low, that is, from one-minute and below. The proposed model, however, may give inaccurate results when used with data sampled at relatively long intervals. For better results, the sampling time should be one-minute and less as recommended by ITU Radiocommunication. Further, the proposed model can be improved by training the BPNN with rain rates of relatively lower sampling time, as low as 10 s. This allows detection of shorter rain spikes for a more accurate link state prediction.

References

[1] E. Matricciani, "Rate of change of signal attenuation from Sirio at 11.6 GHz," *Electronic Letters*, Vol. 17, No. 3, pp. 139-141, Feb. 1981.

[2] G. O. Ajayi and E.B.C. Ofoche, "Some tropical rain rate characteristics at Ile-Ife for microwave and millimeter wave applications," *Journal of Climate and Applied Meteorology*, Vol. 23, pp. 562-567, 1984.

[3] D. L. Emiliani, L. Luini, and C. Capsoni, "Analysis and parameterization of methodologies for the conversion of rain rate cumulative distributions from various integration times to one minute," *IEEE Antennas and Propagation Magazine*, Vol.51, No.3, pp. 70-84, Jan. 2009.

[4] M. N. Ahuna, T. J. Afullo, and A. A. Alonge, "30-second and one-minute rainfall rate modelling and conversion for millimetric wave propagation in South Africa", *SAIEE Africa Research Journal*, Vol. 107, No. 1, pp. 17-29, Mar. 2016.

[5] C. I. Christodoulou, S. C., M. Gabella, and C.S. Pattichis, "Prediction of rainfall rate based on weather radar measurement," *IEEE Proceedings of Int. Joint Conference of Neural Networks*, Vol. 2, pp. 1393-1396, 2004.

[6] K. Abhishek, A. Kumar, R. Ranjan, and S. Kumar, "A rainfall prediction model using artificial neural network," *IEEE Control and System Graduate Research Colloquium*, pp. 82-87, 2012.

[7] D. R. Nayak, A. Mahapatra, and P. Mishra, "A Survey on rainfall prediction using artificial neural network," *International Journal of Computer Applications*, Vol. 72, No. 16, Jun. 2013.

[8] M. N. Ahuna, T. J. Afullo, and A. A. Alonge, "Rainfall rate prediction based on artificial neural networks for rain fade mitigation over earth-satellite link," *IEEE Africon 2017 Proceedings*, 2017, pp. 579-584, Sept. 2017.

[9] S. C. Michaelides, C. C. Neocleous, and C. N. Schizas, "Artificial neural networks and multiple linear regressions in estimating missing rainfall data," in *Proceedings of the DSP95 International Conference on Digital Signal Processing, Limassol, Cyprus*, 1995, pp. 668–673.

[10] K. C. Luk, J. E. Ball, and A. Sharma, "An application of artificial neural networks for rainfall forecasting," *Mathematical and Compuer modelling*, Vol. 33, pp. 683-693, 2001.

[11] N. Q. Hung, M. S. Babel, S. Weesakul, and N. K. Tripathi, "An artificial neural network model for rainfall forecasting in Bangkok, Thailand," *Hydrol. Earth Syst. Sci*., 13, pp. 1413-1425, 2009.

[12] H. D. Purnomo, K. D. Hartomo, and S. Y. J. Prasetyo, "Artifcial neural network for monthly rainfall rate prediction," *1st Annual Applied Science and Engineering Conference*, 180, pp.109, 2017.

[13] G. M. N. French, W. F. Krajewski, and R. R. Cuykendall, "Rainfall Forecasting in space and time using neural network," *J. Hydrol*. Vol. 137, pp. 1-31, 1992.

[14] R. Rojas, "The Backpropagation Algorithm" in *Neural Networks: A systematic Introduction,* Berlin, Germany: Springer-Verlag, 1996, pp. 151-182.

[15] D. E. Rumelhart, G. E. Hinton, and R. J. Williams, "Learning internal representations by error propagation," in *Parallel Distributed Processing*, Vol. 1, J. A. Feldman, P. J. Hayes, D. E. Rumelahart, Eds. London, England: MIT Prss, 1986, pp. 318-362.

[16] F. Moupfouma, "Model of rainfall-rate distribution for radio system design," IEE *Proceedings*, Vol. 132, No. 1, pp. 39-43, Feb. 1985.

[17] ITU-R Recommendation for Characteristics of precipitation for propagation modelling, ITU-R P.837-6, 2012.

[18] G. F. Bryant, I. Adimula, C. Riva, and G. Brussaard, "Rain attenuation statistics from rain cell diameters and heights," *International Journal of Satellite Communication*, Vol. 19, pp. 263-283, 2001.

[19] C. Capsoni, L. Luini, A. Paraboni, C. Riva, and A. Martellucki, "A new prediction model of rain attenuation that separately accounts for stratiform and convective rain," *IEEE Transactions on Antennas and Propagation*, Vol. 57, No. 1, pp.196-204, 2009.

[20] R. K. Crane, "A two-component rain model for the prediction of attenuation statistics," *Radio Science,* Vol. 17, No. 6, pp. 1371-1387, 1982.

[21] E. Matricciani, "Physical-mathematical model of the dynamics of rain attenuation based on rain rate time series and a two-layer vertical structure of precipitation," *Radio Science,* Vol. 31, No. 2., pp. 281-295, Mar. 1996.

[22] ITU-R Recommendation for Propagation and prediction methods required for design of earth-space telecommunication system*s*, ITU-R P.618-13, 2017.

[23] ITU-R Recommendation for Specific attenuation model for rain for use in prediction methods, ITU-R P.838-3, 2005.

[24] E. Matricciani and C. Riva, "The search for the most reliable long-term rain attenuation CDF of a slant path and the impact on prediction models," *IEEE Transactions on antennas and Propagation*, Vol. 53, No. 9, Sept. 2005.

[25] M. N. Ahuna and T. J. Afullo, "Effects of storm attenuation over satellite links in sub-tropical Africa," *Progress In Electromagnetics Research Symposium*, Toyama, Japan, 1st – 4th Aug. 2018.

Mary Ahuna graduated with a B.Phil. Tech. degree in Electrical and Electronic Engineering from the University of Nairobi, Kenya, in 2012. She received her M.Sc. degree in Electronic Engineering from the University of KwaZulu-Natal, South Africa, in 2016. Currently, she is a Ph.D. student at the University of KwaZulu-Natal, in the Discipline of Electrical, Electronic and Computer Engineering.

Her research interests focus on microwave and millimeter wave propagation studies with special interests in the effects of rain on the performance of earth-satellite communication links and dynamic rain fade mitigation techniques.

She is a member of the Institute of Electrical and Electronic Engineers (IEEE), IEEE Women in Engineering and HKN Eta Kappa Nu (Mu Eta Chapter).

Thomas J. O. Afullo received his B.Sc (Hons) in Electrical Engineering from the University of Nairobi, Kenya (1979); the MSEE from West Virginia University, USA (1983); and the Ph.D. degree in Telecommunications from Vrije Universiteit Brussel (VUB), Belgium, (1989). He worked with Kenya Posts and Telecommunication Corporation as Pupil Engineer, Executive Engineer, and Senior Executive Engineerfrom1981-1986. He was with Moi University, Kenya from 1986-1994, from Tutorial Fellow, to Lecturer and Senior Lecturer and Head of Department. He was Lecturer at the University of Botswana (1996- 2002); and Associate Professor, UDW/UKZN, South Africa (2003-2010).

He is Professor of Microwave Engineering in the Discipline of Electrical, Electronic and Computer Engineering, University of KwaZulu-Natal (UKZN), Durban. His research interests include radio wave propagation, antenna design, cognitive radio, and power line communication.

He is a Registered Professional Engineer in South Africa, a Senior Member of IEEE, a Fellow of South African Institute of Electrical Engineers, Faculty Advisor of Eta Kappa Nu (Mu Eta Chapter), and a Rated Researcher with South Africa's national Research Foundation (NRF).

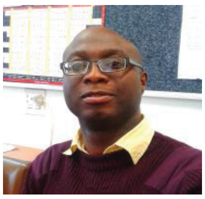

Akintunde Alonge received his B.Eng. (Hons) in Electrical and Electronic Engineering from the Federal University of Technology, Akure, Nigeria in 2007. He thereafter received both his M.Sc. [Eng.] and Ph.D. degrees in Electronic Engineering at the University of KwaZulu-Natal, Durban in 2012 and 2015 respectively.

He is currently a senior lecturer in the Department of Electrical and Electronic Engineering technology at the University of Johannesburg, South Africa.

He is a member of the Institute of Electrical and Electronic Engineers (IEEE). His research interest lies in telecommunication particularly in microwave and millimeter wave systems in relation to futuristic 5G communication systems.